The Journal of the Korean Society of Oceanography
Vol. 30, No. 3, pp. 227-236, June 1995

A multilayer Model for Dynamics of Upper and Intermediate Layer Circulation of the East Sea

YOUNG HO SEUNG AND KUK JIN KIM
Dept. of Oceanography, Inha Univ.
Incheon, 402-751, Korea

동해의 상, 중층 순환 역학에 대한 다층모델

승영호 · 김국진
인하대학교 해양학과

A simple layer model based on isopycnal coordinate is applied to the East Sea to examine the dynamics of circulation. The results confirm the existing knowledge about the role of inflow-outflow and wind in driving the circulation. It is found, however, that the buoyancy flux generates quite different circulation pattern; it enhances the inflow-outflow driven circulation and has a convective nature. The circulation considering all these effects resembles the schematic one presently known. In this circulation, the intermediate layer is outcropped in the north off the northern boundary, ventilated here and flows cyclonically in the northern part of the basin. This water, however, does not flow southward directly because of the strong eastward (separating from the coast) current in the layer above. This water also loses its potential vorticity while traveling around the periphery of the outcropping region and is thus characterized by minimum potential vorticity in the interior of the basin.

동해의 해수순환 역학을 규명하기 위하여 등밀도 좌표계에 근거한 다층모델을 적용하였다. 모델결과, 유입-유출과 바람에 의한 기존의 역할을 확인할 수 있었다. 그러나 해양-대기 열교환에 의한 영향은 다르게 나타났다. 즉, 열교환에 의해 유입-유출 효과가 강화되고 대류형의 순환이 생성되었다. 상기의 세가지 요인을 모두 고려했을시의 순환형태는 기존의 모식도와 흡사하였다. 이 순환에서는 중층수가 북쪽에서 표면 노출되었으며 이 곳에서 벤틸레이숀 효과로 인하여 반시계 방향의 중층순환을 형성하였다. 그러나 이 중층수는 표층부근의 강한 서향류로 인하여 연안을 따라 직접 남하하지는 못하는 것으로 나타났다. 또 북쪽의 반시계 순환 중 계속하여 포텐샬 와도를 잃음으로써 와도 최소수를 만드는 것으로 나타났다.

INTRODUCTION

Most of the East Sea basin is filled with a very thick, cold and nearly homogeneous water, called the Japan Sea Proper Water (JSPW). There have been many questions about the formation and circulation of the JSPW and many of them still remain unknown. The presence of oxygen-rich East Sea Intermediate Water (ESIW) in the upper part of the JSPW (Uda, 1934; Kim & Chung, 1984; Kim et al., 1991) also indicates that it is continuously renewed somewhere. In fact, there is an evidence of deep winter convection in the northwestern part of the basin (Seung & Yoon, 1995a). Senjyu and Sudo (1994) also analysed the historical data to show that the upper portion of the JSPW extending over the whole basin originates from the northwest. They also suggested that the newly formed water mass circulates around the basin anti-clockwise.

Overlying the ESIW, there is a shallow surface

layer, called the Tsushima Current Water (TCW), entering the Korea Strait and flowing out through the Tsugaru and Soya Straits (Fig. 1). A part of it flows along the Japanese coast due to the topographic control (Yoon, 1982b), the so called Nearshore Branch (NB), and much of it flows northward along the Korean Coast, forming the East Korean Warm Current (EKWC). The EKWC separates from the coast near 38° N, then orients toward the outlet across the basin. North of the warm current region, a cold current called the North Korean Cold Current (NKCC) and Liman Current (LC) flows southward along the western boundary and the former separates from the coast where it meets with the EKWC. Most of these schematic features are generally confirmed by numerical models (Yoon, 1982a and b; Seung and Kim, 1993; Seung and Yoon, 1995b).

Seung (1992) has analysed the circulation dynamics of upper layer and pointed out the importance of local forcing in controling separation of the EKWC and formation of the NKCC. It, however, has only one moving layer above the infinitely deep motionless layer and does not allow the outcropping of the layer interface. It, therefore, cannot resolve any three dimensional nature of circulation such as ventilation and subduction of cold water below the warm upper layer. In this study, we treat the same problem with exploring the three-dimensional feature of circulation. We are especially interested in the behavior of the ESIW just beneath the moving TCW. As mentioned earlier, the ESIW found over the basin is assumed to be formed in the north/northwest. The employed model has very simple dynamics but uses isopycnal coordinate allowing the outcropping of isopycnal surfaces, which is quite suitable for analyzing the dynamics of circulation with convective nature. We first give a brief description of the model, then discuss the model results and finally draw some conclusions.

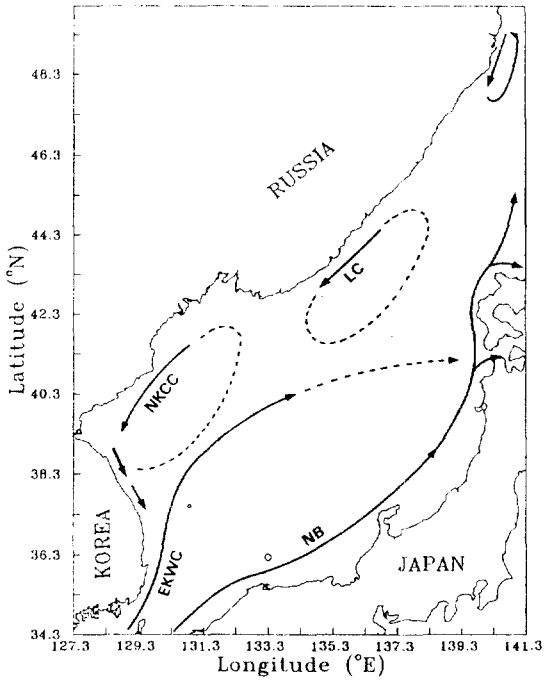

Fig. 1. A schematic diagram of the East Sea circulation (after Uda, 1934). LC means Liman Current; NKCC, North Korean Cold Current; EKWC, East Korean Warm Current; NB, Nearshore Branch. The EKWC and NB enter through the Korea Strait and flows out through the Tsugaru (south) and Soya (north) Straits.

MODEL

The model is the same as that used by Huang and Bryan (1987) except that some modifications are made for application to the East Sea. The original model has a mixed layer with fixed constant depth and, below it, two moving layers with variable depths. The lowest layer is assumed infinitely deep and motionless. The horizontal motion is driven by both the surface wind stress and buoyancy flux. The latter is parameterized by simple newtonian density flux, $\gamma(\rho^*-\rho_1)$, where: γ is the flux coefficient; ρ_1, the mixed layer density; and ρ^*, the reference density. The induced motion is modified by friction between layers and horizontal eddy viscosity, which otherwise is geostrophic. In the mixed layer, the density value is updated and, below it, the layer thickness are updated. In the latter process, the density coordinate and flux-corrected-transport scheme (Zalesak, 1979) are employed. Convective adjustment induced by surface cooling is done in such a way that total volume and buoyancy are unchanged. For more detailed description, refer to

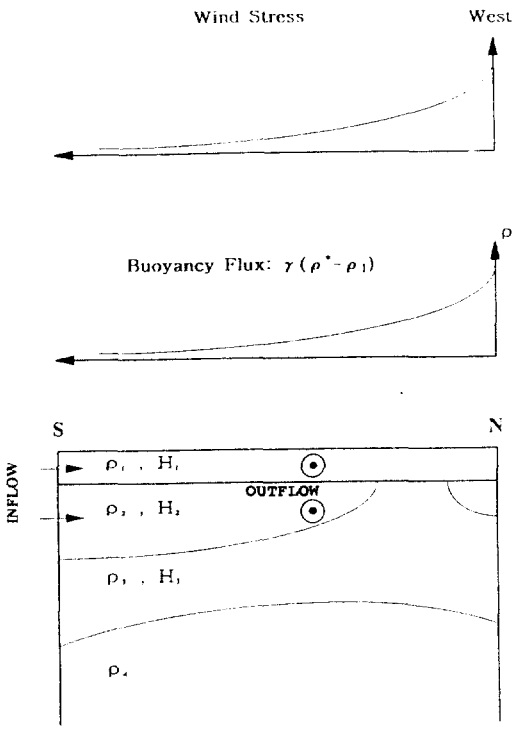

Fig. 2. Definition sketch of the model. ρ_i and H_i mean density and layer thickness, respectively, of i_{th} layer. The model is forced from above by a zonal exponential wind and a buoyancy forcing represented by a reference density ρ^* of exponential type. It is also driven by inflow-outflow imposed on the mixed and second layers.

Huang and Bryan (1987).

In this study, the model East Sea is assumed for convenience a rectangle with dimension 1200×1500 km in east-west and north-south directions, respectively; this area is covered by 26×32 grid squares of size 50km. The simplification of basin geometry is not serious because we are satisfied with only the qualitative feature of dynamics. Vertically, the basin consists of 4 layers: mixed layer with depth 50 m, second layer with density ρ_2=1026.21 kg/m^3 representing the layer of TCW, third layer with density ρ_3=1026.87 kg/m^3 representing the layer of ESIW and infinitely deep and motionless fourth layer with density ρ_4=1027.36 kg/m^3 representing the JSPW (Fig. 2).

Differently from Huang and Bryan's model, inflow and outflow through open boundaries are imposed in the mixed and second layers. The amount of transport is 0.75 Sv in the mixed layer and 1.5 Sv in the second layer. It is reminded that the volume transport of Tsushima Current varies from 1 to 3 Sv (Yi, 1966; Miita & Ogawa, 1984). The current at the inflow opening is assumed geostrophic and infinitely fast radiation is assumed at the outflow opening. The wind stress curl is taken to have the same form as that in Seung (1992), i.e. southward exponential decrease of positive stress curl with scale comparable to the dimension of the basin (Fig. 2). If we consider only the zonal component of wind stress, it becomes

$$\tau^x = -\tau_o \, e^{(y - y_N)/L} \tag{1}$$

where: τ^x is the x-component of wind stress: τ_o, the magnitude of wind stress; y_N, the y-position of the northern boundary; and L (=1500 km) is the meridional dimension of the basin. The wind stress shown in (1) may not be realistic but it is not serious because only the stress curl is important rather than the stress itself. According to Na et al. (1992), the maximum wind stress curl, τ_o/L, is about 10^{-7} N/m^3 ($=10^{-8}$ dyne/cm^3) and occurs in the north; we take τ_o = 0.1 N/m^2 here. The reference state density, ρ^*, in the surface buoyancy flux is also assumed to have the same exponential type (Fig. 2) as follows:

$$\rho^* = \rho_E + (\rho_N - \rho_E) \, e^{(y - y_N)/L} \tag{2}$$

where: ρ_E (=1026.15 kg/m^3) is the mixed layer density at the inflow opening and ρ_N is the value of ρ^* at $y=y_N$. The value ρ_N should be greater than ρ_2 for the third layer to outcrop but smaller than ρ_3 for the fourth layer not to outcrop, which case is the one we are interested. The flux coefficient γ is also important as well as ρ^* in controlling the amount of buoyancy flux. Various values of ρ_N and γ were tried and the most acceptable result is obtained with ρ_N=1026.75 kg/m^3 and $\gamma = 5 \times 10^{-4}$ sec^{-1}. The latter has a time scale of 1000 seconds which is shorter than those generally used in large-scale ocean circulation. Eddy viscosity coefficients and friction coefficients do not play the major role in the dynamics; we take the horizontal and vertical eddy viscosity coefficients A_H and A_Z as 1×10^4 m^2/sec

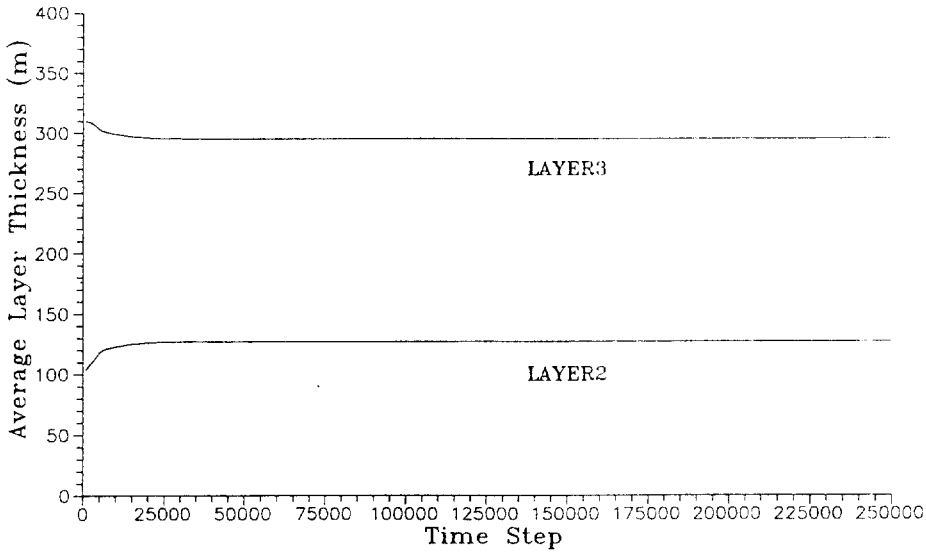

Fig. 3. Time series of layer thickness. One time step is 3600 seconds.

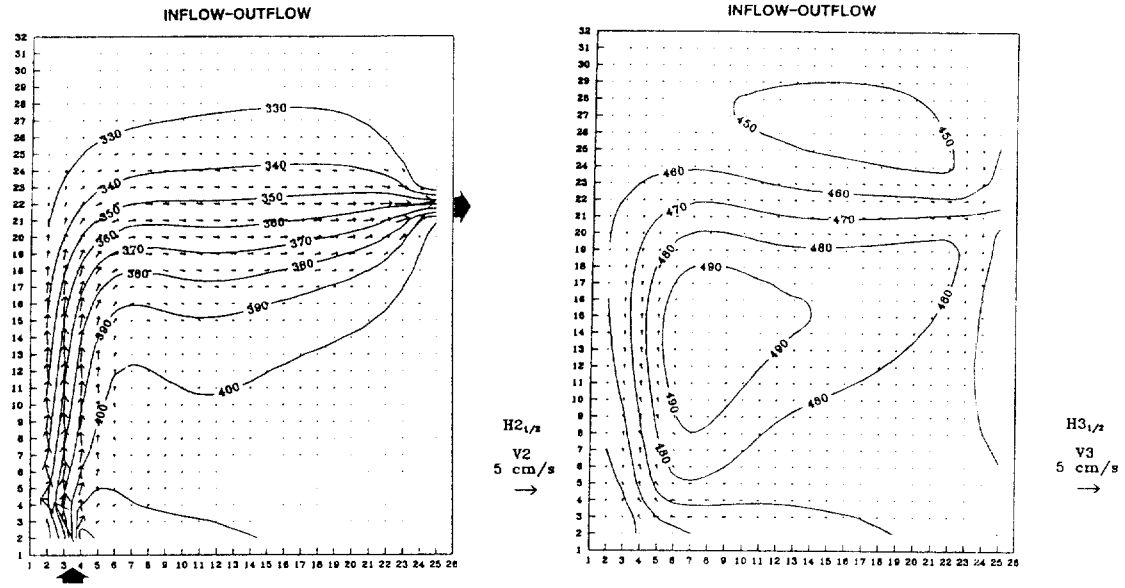

Fig. 4. Current arrows and contours of layer bottom depth (in meter) for second (left, layer bottom depth $H_{2\frac{1}{2}}$) and third (right, layer bottom depth $H_{3\frac{1}{2}}$) layers for the case of model forced by inflow-outflow. Thick arrows mean inflow and outflow.

and 10^{-4} m^2/sec, respectively, and the interfacial friction coefficient k as 2×10^{-4} m/sec. The model with these parameters gives quick steady state results (Fig. 3).

RESULTS

As in Seung (1992), we examine first the roles of three factors in driving the circulation, i.e. inflow-

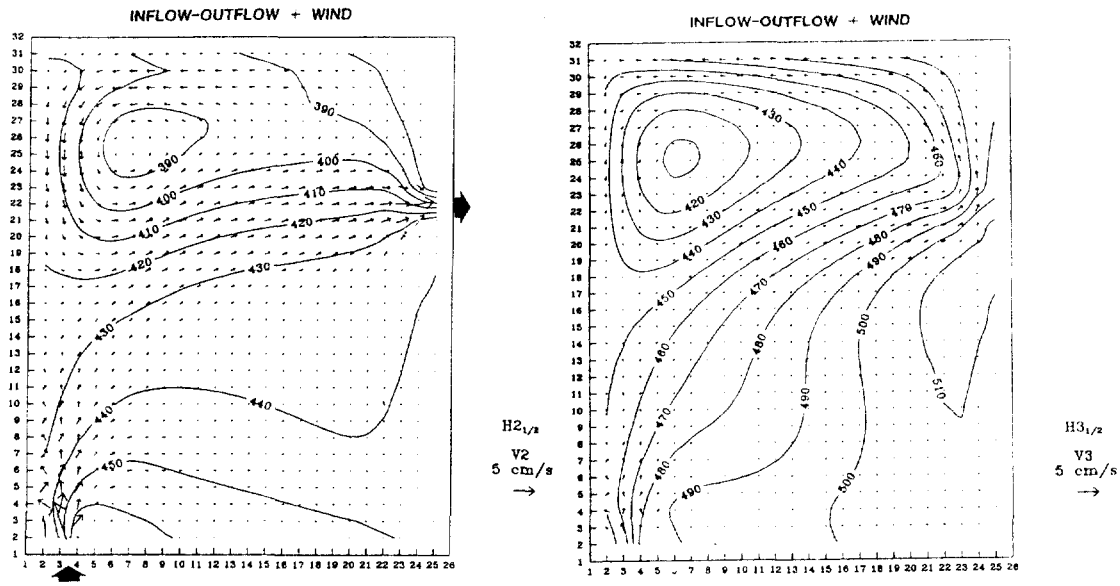

Fig. 5. Same as Fig. 4 except for the model forced by inflow-outflow and wind.

outflow, surface wind stress curl and surface buoyancy flux. The circulation driven by inflow and outflow (Fig. 4) shows nearly the same feature as the one obtained in the previous quasi-geostrophic model (Seung, 1992, Fig. 3): it consists of a western boundary current (EKWC) and a zonal current flowing toward the outlet. The separation of the EKWC occurs at the same latitude as the outlet. This pattern also occurs in the third layer below. In the third layer where no opening presents, however, broad return currents present, forming an anticyclonic gyre in the south and a smaller cyclonic gyre in the north.

When wind is imposed, a cyclonic gyre develops in the north (Fig. 5). The circulation driven by inflow-outflow is largely disturbed in such a way that it becomes less organized and the separation point is suppressed southward. It has been already pointed out (Seung, 1992) that wind, with positive stress curl, creates cyclonic gyre in the north and suppresses southward the separation point. The circulation patterns are nearly the same between second and third layers except that in the latter some recirculation develops due to the absence of the openings.

Contrary to the wind, the buoyancy flux gives the circulation quite different from that obtained in previous model (Fig. 4 in Seung, 1992). This fact can be observed by comparing the two circulations driven by inflow-outflow with and without buoyancy flux (Fig. 4 and Fig. 6). In the second layer, the circulation driven by buoyancy flux seems nearly the same as that by inflow-outflow, thus enhancing the latter. After crossing the basin eastward, it continues to flow northward along the eastern boundary. It ends slowly near the northeastern corner. On the contrary, a southward current suddenly appears at the same location below in the third layer. This fact suggests that the second layer water carried to the northeast sinks there, then flows back to the south in the third layer; part of it slowly upwells to the second layer, forming a closed convective circulation. The third layer also outcrops extensively in the north/northwest.

The circulation in the second layer with all these factors included (Fig. 7) resembles the schematic one except the NB which is controlled by bottom topography and not considered in this model (Fig. 1). The outcropping of the third layer created by the buoyancy flux is largely modified by the wind. It is noted that the outcropping does not occur along the northern boundary despite the most intense buoyancy flux in this region. It seems that the amount of

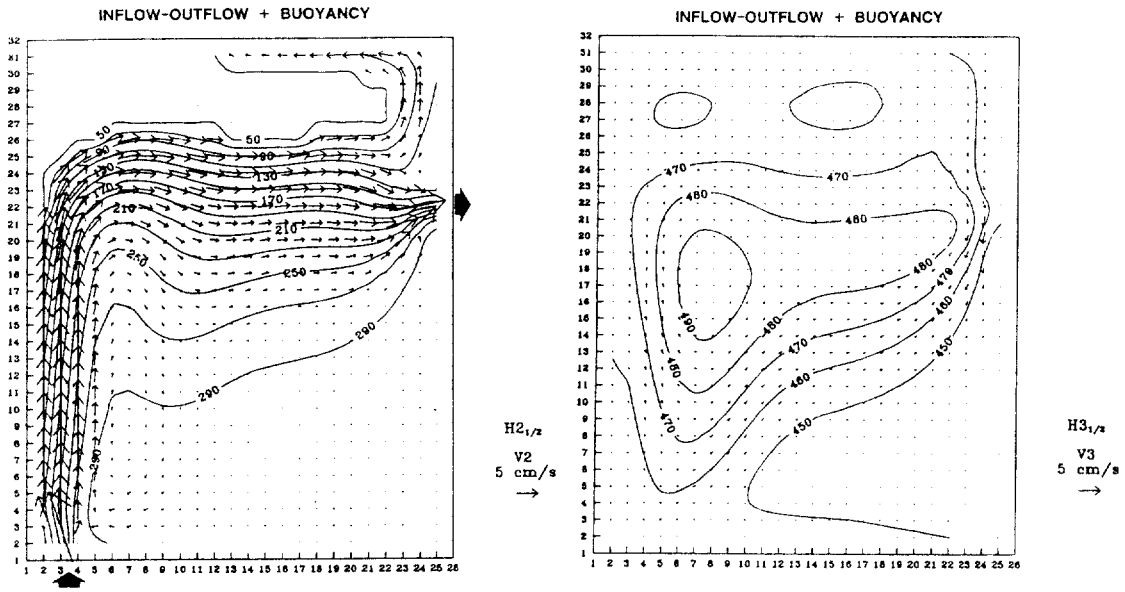

Fig. 6. Same as Fig. 4 except for the model forced by inflow-outflow and buoyancy flux. The region enclosed by isobath 50 m is outcropped.

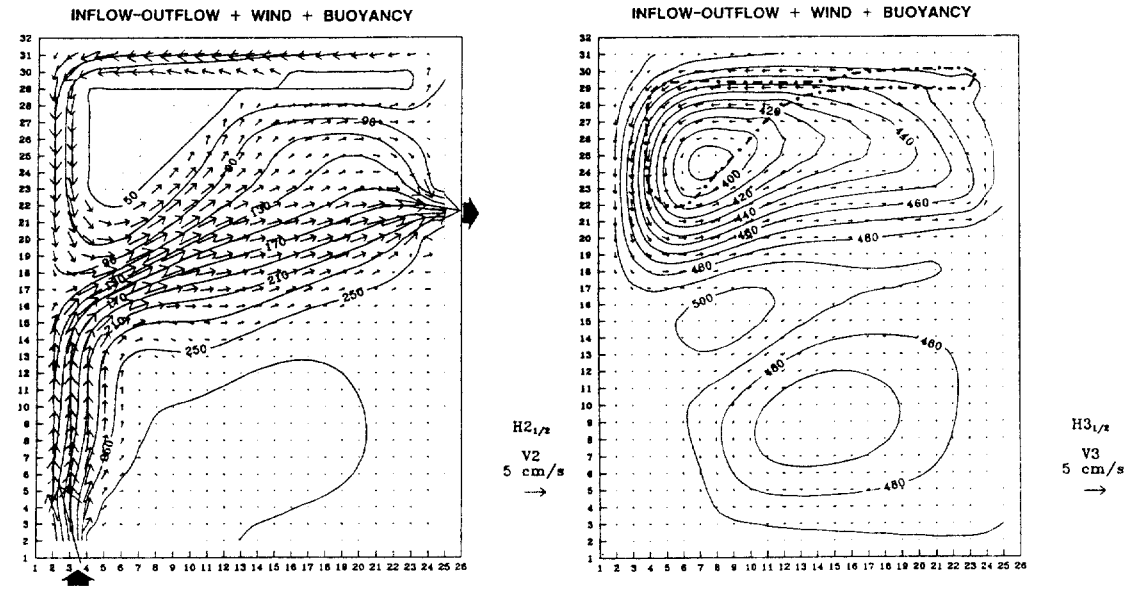

Fig. 7. Same as Fig. 6 except for the model forced by inflow-outflow, wind and buoyancy flux. Thick dotted line is the boundary of outcropped region.

water carried here by the effect of wind is larger than that transformed into the lower layer water by the buoyancy flux. In the third layer, two cyclonic gyres dominate the whole basin: a strong one in the north and a weak one in the south. This circulation pattern seems to be created mostly by the wind with positive stress curl which becomes more pronounced by the effect of buoyancy flux. The wind

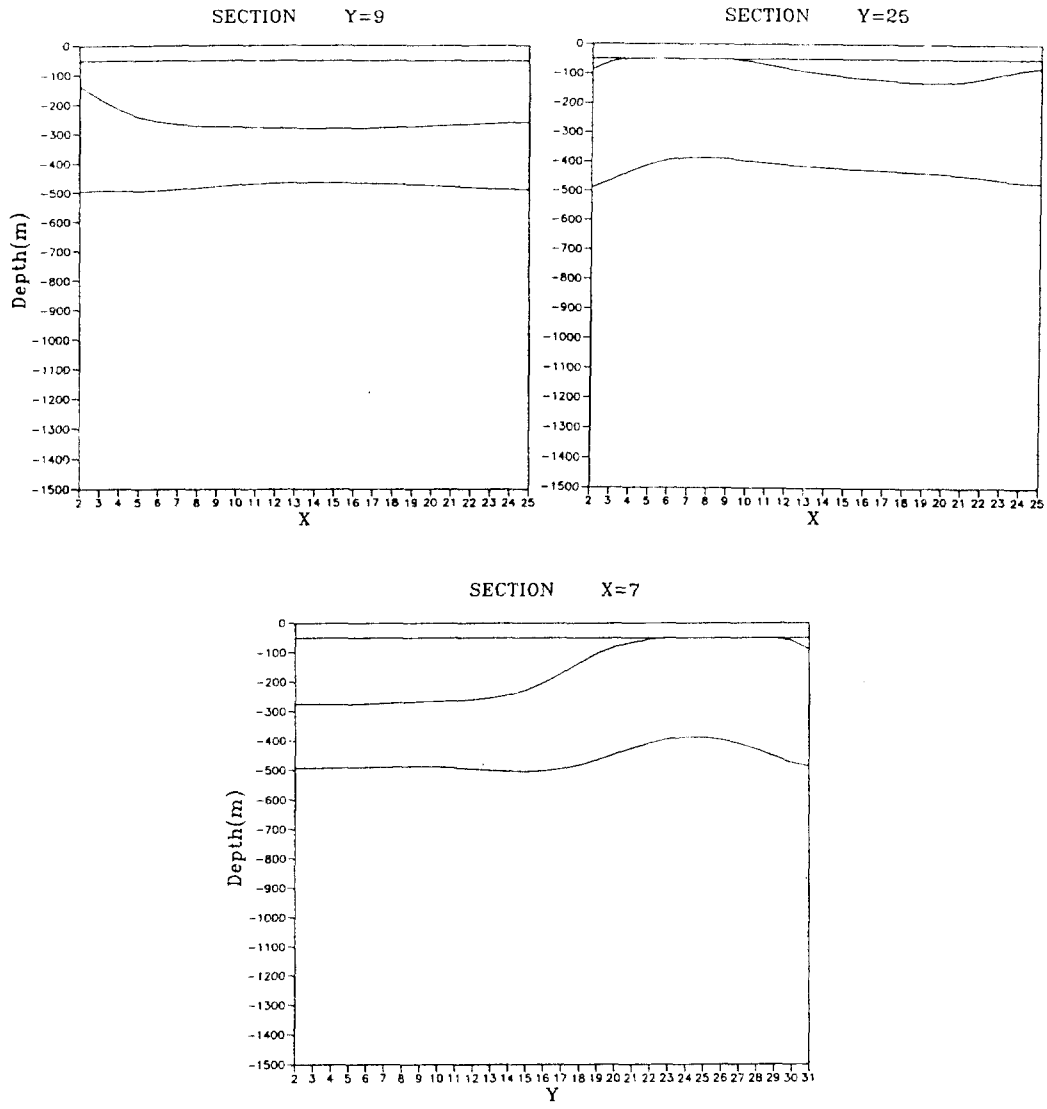

Fig. 8. Vertical sections along the zonal lines y=9 and y=25, and the meridional line x=7. Refer to previous figures for (x, y) coordinates.

effect can be transferred into the third layer more effectively through the outcropped region and then spread beneath the upper layer over the basin, i.e., the third layer is ventilated. The separation of the otherwise single large cyclonic gyre into two gyres seems to be due to the strong current above, crossing the basin from the separation point toward the outlet. A strong gradient in water column thickness (thus potential vorticity) develops across this current which then acts as a barrier on the movement of water in the third layer.

Currents in upper and lower layers are in good geostrophic balance as seen from the fact that each current runs approximately parallel to the isopleths of corresponding layer bottom depth; the interface between third and fourth layers coincides with the isobaric surface and that between second and third layer may be considered so if the current (pressure

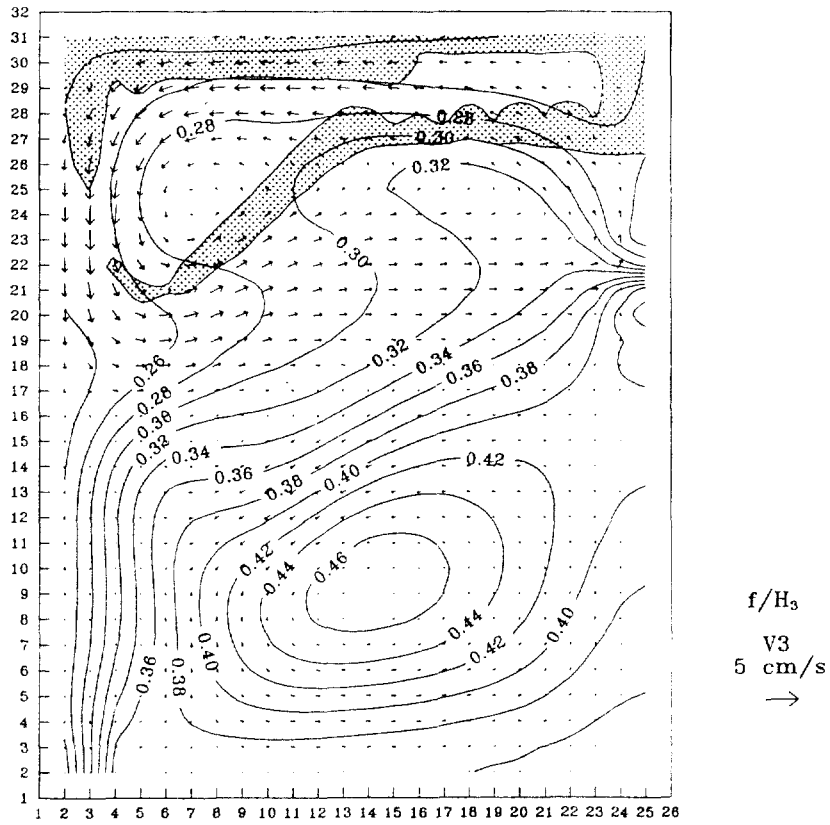

Fig. 9. Distribution of potential vorticity f/H_3(in 10^{-6} m^{-1} sec^{-1}) and currents in third layer. Large water mass conversion (larger than 3×10^{-6} m/sec) occurs within the shaded area.

gradient) in the third layer is much smaller than that in the second layer. Geostrophy of the current can be seen also from the vertical sections across the basin (Fig. 8). The doming and slope of the interfaces associated with the northern cyclonic gyre and strong current, respectively, are the manifestations of geostrophy. Veering of current occurs in the northern interior of the basin south of the outcropping region. For quasi-geostrophic current, anti-clockwise veering (in upward direction) is associated with downward vertical velocity at the interface of two layers and vice versa. The current following the isopleths 110-210m of the interface between the second and third layers has relatively large downslope component, thus associated with the anti-clockwise veering.

Distribution of the potential vorticity (Fig. 9) in the third layer indicates that the intermediate water (third layer) loses its potential vorticity while traveling along the periphery of the outcropping zone. It gains again its potential vorticity as it ejects offshore from the western boundary. Change of potential vorticity is largely determined by the change of water column thickness. The loss of potential vorticity around the periphery of the outcropping region seems therefore to be associated with water mass conversion by convective adjustment (increase of water column thickness) which also occurs around the periphery. The loss of potential vorticity is usually observed in the area of deep/intermediate water formation in the open ocean (McDowell et al., 1982; Talley & McCartney, 1982). The retrieval of potential vorticity offshore the western boundary is related to the downslope current mentioned earlier, thus

shrinking of water column. However, it is not known how the local forcing interferes in this process.

CONCLUDING REMARKS

This study considers the previous problem (Seung, 1992) using three dimensional model and thus allows the outcropping of the intermediate layer in the north of the basin. The three factors controling the circulation are reexamined. The inflow-outflow and wind have nearly the same effects on the circulation as those in the previous two-dimensional case. The former generates a western boundary current and a zonal current toward the outlet; the western boundary current separates from the coast at the same latitude as the outlet. The latter creates a cyclonic recirculation gyre in the north and suppresses the separation position of the western boundary current southward. The effect of buoyancy, however, is quite different from that in the previous two dimensional case. It creates the western boundary current, separation of this, a zonal current and an eastern boundary current flowing northward. This current involves a sinking in the northeastern part and broad upwelling in the southwestern part after being transported southward by a return current in the layer below. The buoyancy thus enhances the circulation driven by inflow-outflow. When inflow-outflow, wind and buoyancy are all present, the circulation of the upper layer resembles the schematic one known presently. In the center of the northern cyclonic gyre, offshore the northern boundary, the intermediate layer outcrops. This layer is thus ventilated through this outcropping region and the cyclonic motion extends far below the upper layer. The southward transport of this intermediate water, however, is largely blocked by the presence of potential vorticity barrier created by the strong zonal current (EKWC separated from the coast) above. Only a small portion of this water is transported southward through the eastern side of the basin. This fact indicates that the ESIW found south of the polar front (or south of the separated EKWC) off the Korean coast (e.g. Kim and Chung, 1984) does not come directly from the north. The intermediate water are formed by water mass conversion around the periphery of the outcropping region. This increases the thickness of water column and thus diminishes the potential vorticity. Consequently, it becomes to have the minimum potential vorticity when it ejects offshore from the western boundary after finishing the cyclonic journey along the periphery of the outcropping region. The potential vorticity so lost is restored when the water column undergoes shrinking after coming out of the western boundary.

The study is by no means complete and its results cannot be taken as definitive. The model is so simple that there might be some important factors which are not taken into consideration. Among them, the inclusion of moving bottom layer with variable bottom topography may significantly change the results and should be attempted in future studies. Though there are many other unrealistic conditions, it is reminded that we are satisfied here with only the qualitative feature of the problem. Among others, this study demonstrates the need and usefulness of layer model based on isopycnal coordinate in understanding the East Sea circulation dynamics especially when it is concerned with the surface buoyancy forcing. This study is thus a first attempt to apply the isopycnal coordinate-based layer model to the East Sea circulation and more complete and realistic one is under consideration.

ACKNOWLEDGEMENT

This paper was supported by NON DIRECTED RESEARCH FUND, Korea Research Foundation (1994) and, in part, by Basic Science Research Institute Program, Ministry of Education (1994). The authors thank to Dr. R. X. Huang for sending a copy of source program of the model and to the referees for kind comments.

REFERENCES

Huang, R. X. and K. Bryan, 1987. A multilayer model of the thermohaline and wind-driven ocean circulation. J. Phys. Oceanogr., **17**: 1909-1924.

Kim, C. H., H. J. Lie and K. S. Chu, 1991. On the In-

termediate Water in the southwestern East Sea (Sea of Japan). "Oceanography of Asian Marginal Seas", ed. K. Takano, Elsevier, Amsterdam, 129-141.

Kim, K. and J. Y. Chung, 1984. On the salinity-minimum and dissolved oxygen-maximum layer in the East Sea (Sea of Japan). "Ocean hydrodynamics of the Japan and East China Seas", ed. T. Ichiye, Elsevier, Amsterdam, 55-65.

McDowell, S., P. Rhines and T. Keffer, 1982. North Atlantic potential vorticity and its relation to the general circulation. J. Phys. Oceanogr., **12**: 1417-1436.

Miita, T. and Y. Ogawa, 1984. Tsushima Currents measured with current meters and drifters. "Ocean hydrodynamics of the Japan and East China Seas", ed. T. Ichiye, Elsevier, Amsterdam, 67-76.

Na, J. Y., J. W. Seo and S. K. Han, 1992. Monthly-mean sea surface winds over the adjacent seas of the Korea Peninsula. J. Oceanol. Soc. Korea, **27**(1): 1-10.

Senjyu, T. and H. Sudo, 1994. The Upper Portion of the Japan Sea Proper Water; Its source and circulation as deduced from isopycnal analysis. J. Oceanogr., **50**: 663-690.

Seung, Y. H., 1992. A simple model for separation of East Korean Warm Current and formation of North Korean Cold Current. J. Oceanol. Soc. Korea, **27**(3): 189-196.

Seung, Y. H. and K. Kim, 1993. A numerical modeling of the East Sea circulation. J. Oceanol. Soc. Korea, **28**(4): 292-304.

Seung, Y. H. and J. H. Yoon, 1995a. Some features of winter convection in the Japan Sea. J. Oceanogr., **51**: 61-73.

Seung, Y. H. and J. H. Yoon, 1995b. Robust diagnostic modeling of the Japan Sea circulation. J. Oceanogr. (in press)

Talley, L. D. and M. S. McCartney, 1992. Distribution and Circulation of Labrador Sea Water. J. Phys. Oceanogr., **12**: 1189-1205.

Uda, M., 1934. Oceanographic conditions of the Japan Sea and its adjacent waters. J. Imp. Fisher. Exp. St., **7**: 91-191. (in Japanese).

Yi, S. U., 1966. Seasonal and secular variations of the water volume transport across the Korea Strait. J. Oceanol. Soc. Korea, **1**: 7-13.

Yoon, J. H., 1982a. Numerical experiment on the circulation in the Japan Sea. Part I: Formation of the East Korean Warm Current. J. Oceanogr. Soc. Japan, **38**: 43-51.

Yoon, J. H., 1982b. Numerical experiment on the circulation in the Japan Sea. Part III: Mechanism of the Nearshore Branch of the Tsushima Current. J. Oceanogr. Soc. Japan, **38**: 125-130.

Zalesak, S. T., 1979. Fully multidimensional flux-corrected transport algorithms for fluids. J. Comput. Phys., **31**: 335-362.

Accepted June 14, 1995